GLUEBALL AND MESON SPECTROSCOPY WITHIN THE GRAVITON SOFT-WALL MODEL*

Matteo Rinaldi

INFN Section of Perugia, Italy

Received 31 January 2023, accepted 1 May 2023, published online 27 October 2023

The main predictions of the so-called Graviton Soft-Wall Model (GSW) are presented. The calculations of hadronic (scalar, vector, pseudoscalar, and axial mesons) and glueball spectra will be discussed together with the mixing conditions. Moreover, a detailed analysis of quantities related to the pion has been also shown. The main outcome of these investigations is that the GSW model is capable to describe very different features of different hadrons and glueballs with only few parameters, thus unveiling his impressive predicting power.

DOI:10.5506/APhysPolBSupp.16.8-A18

1. Introduction

Here, the recent predictions of the so-called Graviton Soft-Wall Model (GSW) [1–5] have been recalled. This approach has been used to describe non-perturbative features of glueballs and hadrons. Holographic-inspired approaches rely on a correspondence between a five-dimensional classical theory with an AdS metric and a supersymmetric conformal quantum field theory. Since the latter is not QCD, we use the so-called "bottom-up" approach [6, 7], where the five dimensional classical theory is properly modified to reproduce non-perturbative QCD properties as much as possible. The GSW model is a modification of the initial soft-wall (SW), see *e.g.* Refs. [7–10], where a dilaton field is introduced to softly break conformal invariance. In the GSW case, a modification of the metric has been proposed. This model has been used to reproduce the spectra of glueballs, scalar, pseudoscalar, and vector mesons [2]. In Ref. [5], quantities related to the pion have been calculated reproducing well the data. Finally, we discussed the mixing condition between scalar glueballs and mesons [3, 11, 12].

* Presented at *Excited QCD 2022*, Sicily, Italy, 23–29 October, 2022.

2. Essential features of the GSW model

The essential difference between the GSW model and the traditional SW one is a deformation of the AdS metric in 5 dimensions

$$ \mathrm{d}s^2 = \mathrm{e}^{\alpha k^2 z^2} g_{MN}\, \mathrm{d}x^M \mathrm{d}x^N = \mathrm{e}^{\alpha k^2 z^2} \frac{R^2}{z^2} \left(\eta_{\mu\nu}\, \mathrm{d}x^\mu\, \mathrm{d}x^\nu - \mathrm{d}z^2\right) , \qquad (1) $$

where g_{MN} is the AdS$_5$ metric [1, 8, 9, 13, 14]. Modifications of the metric have been also proposed in other studies of the properties of mesons and glueballs within AdS/QCD [8, 14, 15]. The action, in the gravity sector, written in terms of the standard AdS metric of the SW model, is

$$ \bar{S} = \int \mathrm{d}^5 x\, \mathrm{e}^{k^2 z^2 \left(\frac{5}{2}\alpha - \beta + 1\right)}\, \mathrm{e}^{-\phi_n(z)} \sqrt{-g}\, \mathrm{e}^{-k^2 z^2} \mathcal{L}(x_\mu, z)\, . \qquad (2) $$

The parameter α encodes the effects due to the modification of the metric, while β is used to recover the kinetic term of the SW action [1, 3, 4]. For scalar fields, $\beta = \beta_s = 1 + \frac{3}{2}\alpha$ and for a vector, $\beta = \beta_v = 1 + \frac{1}{2}\alpha$. In Ref. [2], an additional dilaton ϕ_n has been included to obtain binding potentials. This quantity does not contain any free parameter. In order to properly take into account the chiral symmetry breaking, the model has been properly modified in Ref. [5].

3. The glueball as gravitons within the GSW model

The GSW model [1] predicts that the scalar and tensor glueballs are described by the graviton which is a solution of the Einstein equation for a perturbation metric (1). The only free parameter is the scale factor $\alpha k^2 \sim (0.37\ \mathrm{GeV})^2$ in Eq. (1). This term is fixed from the comparison with lattice QCD [1] (see the left panel of Fig. 1). We also stress the good agreement with the ground-state mass obtained by the BESIII data of the J/Ψ decays [16, 17].

4. Scalar spectra

As in the SW model, we study the modes of scalar fields propagating in the space, Eq. (1) [8, 15, 18]. In this case, the action is [4]

$$ \bar{S} = \int \mathrm{d}^5 x\, \sqrt{-g}\, \mathrm{e}^{-k^2 z^2 - \phi_n} \left[g^{MN} \partial_M S(x) \partial_N S(x) + \mathrm{e}^{\alpha k^2 z^2} M_5^2 R^2 S(x) \right] . \qquad (3) $$

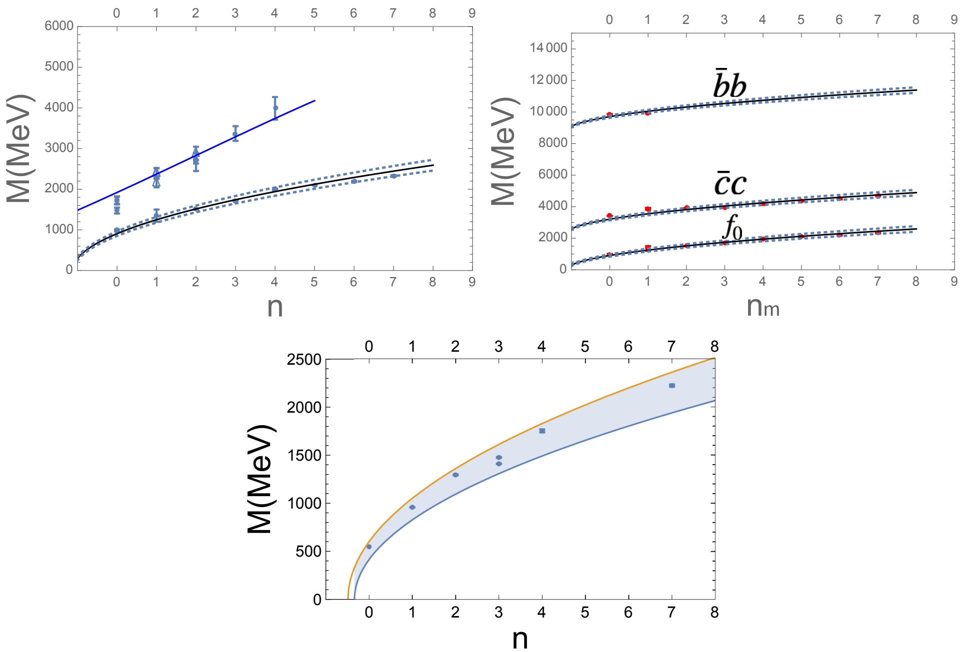

Fig. 1. Top left: GSW fit to the lattice glueball spectrum (upper line) and to the experimental scalar meson spectrum (lower line). Dotted lines for variation of α. Top right: GSW fit to the data for all quark sectors. Bottom: the η spectrum. Data references in Ref. [2].

4.1. Glueballs

For glueball with even spin of odd spin J, $M_5^2 R^2 = (J+2)(J+6)$. Since $M_5^2 R^2 \geq 0$, the potential will bind, then $\phi_n = 0$ (2). Results of the calculations, in fairly agreement with data as summarized by the Regge trajectories: $J \sim (0.18 \pm 0.01)M^2 - 0.75 \pm 0.28$ in agreement with $J \sim 0.18M^2 + 0.25$ [19].

4.2. Light, heavy, and pseudo-scalar mesons

In this case, $M_5^2 R^2 = -3$ in Eq. (3). Here, the relative potential is not binding. Therefore, the additional contribution $\phi_n(z) \neq 0$, see details in Ref. [2]. We only mention that ϕ_n is chosen to produce the potential obtained by expanding $\exp(\alpha k^2 z^2)$ in Eq. (3) up to the second order. By keeping fixed $\alpha k^2 = 0.37$ GeV^2, a reasonable good fit is found (see the left panel of Fig. 1) for $0.51 \leq \alpha \leq 0.59$. In the case of heavy mesons, we added the quark mass contributions to the light scalar masses [2, 4, 20, 21]. The heavy mass (M_h) is obtained from the light one (M_l) as follows: $M_\mathrm{h} = M_\mathrm{l} + C$, where C is the contribution of the heavy-quark masses. $C_c = 2400$ MeV for the $c\bar{c}$ mesons, and for the $b\bar{b}$ mesons $C_b = 8700$ MeV (close to the physical masses). The successful comparison with data [4] is displayed in the top right panel of Fig. 1. For the pseudo-scalar, $M_5^2 R^2 = -4$ [22]. In the bottom panel of Fig. 2, we show our calculation of the spectrum. The comparison with the experimental data is very good. Moreover, the GSW model predicts that $\eta(1405)$ and $\eta(1475)$ are degenerate, as discussed in the PDG review, and *(i)* the existence of two resonances between the $\eta(1760)$ and $\eta(2225)$, and *(ii)* that the $\eta(1405)$ and $\eta(1470)$ are the same resonance.

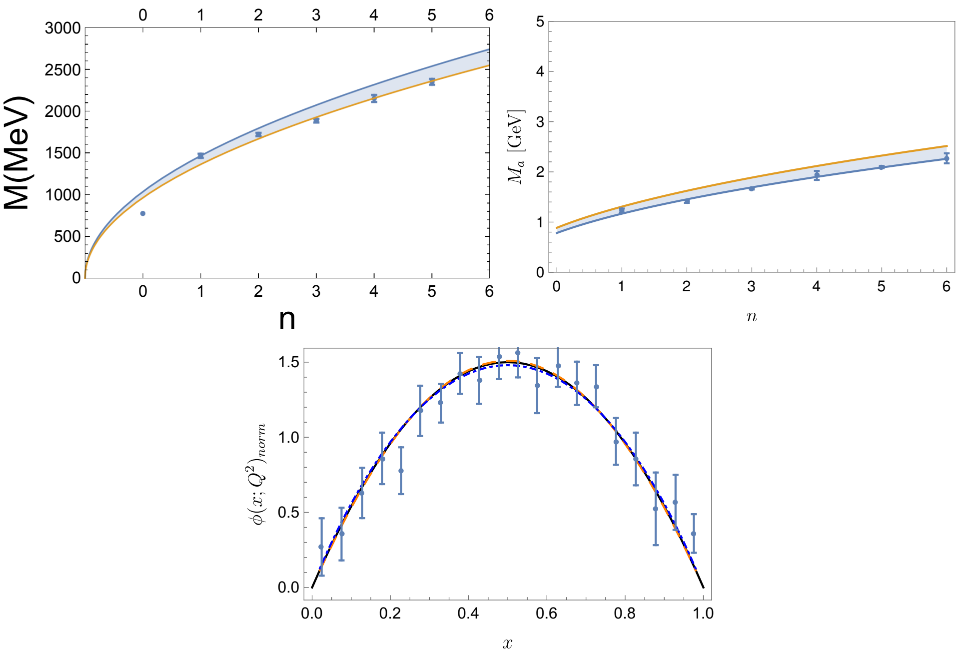

Fig. 2. Top left: The ρ mass plot as a function of mode number. Top right: the a_1 spectrum. Bottom: the pion normalized DA evolved at $Q = 3.16$ GeV [5]. All data references are included in Refs. [2, 5].

5. Vector fields

The action for a vector field reads [15]

$$\bar{S} = -\int \mathrm{d}^5 x \frac{\sqrt{-g}}{2}\, \mathrm{e}^{-k^2 z^2 - \phi_n} \left[\frac{1}{2} g^{MP} g^{QN} F_{MN} F_{PQ} + M_5^2 R^2 g^{PM} A_P A_M \,\mathrm{e}^{\alpha k^2 z^2} \right] . \tag{4}$$

For the ρ meson, $M_5^2 R^2 = 0$ and $\phi_n = 0$ [15]. As one can see in the top left panel of Fig. 2, the agreement is good, exception is $\rho(770)$. In the case of the axial-vector mesons, due to chiral symmetry breaking, $M_5^2 R^2 = -1$ [22, 23], thus a modification of the dilaton is required [2]. With the parameters previously addressed, we get the spectrum shown in the top right panel of Fig. 2. Our calculation favors that the $a_1(1930)$, $a_1(2095)$ and $a_1(2270)$ are axial resonances and a missing ground state with a mass lower than the quoted 1230 MeV.

5.1. The pion structure

In the case of the pion, we need to incorporate into the model the chiral symmetry breaking mechanism. To this aim, in Ref. [5] we propose the following strategy. We first impose that the additional dilaton ϕ_n ensures that the pion is massless due to chiral symmetry. To this aim, a parameter γ_π has been introduced. Then, in order, to break this symmetry, we followed the lines of Ref. [24] where the longitudinal dynamics has been introduced. Details can be found in Ref. [5]. Let us mention that at the end two free parameters are requested: γ_π and the quark mass m_q. We prosed two ansatze: $\gamma_\pi = -0.6$ (-0.17) and $m_q = 45$ (52) MeV called GSWL1 (GSWL2). Both

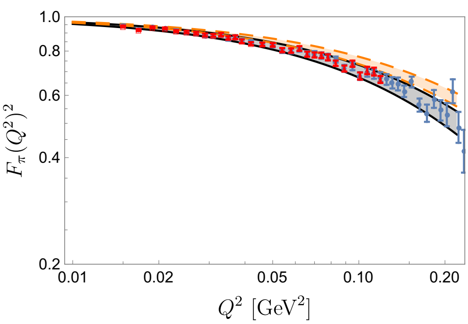

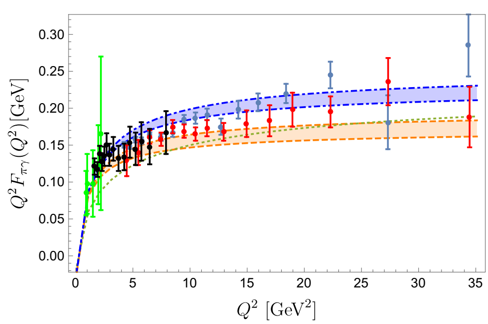

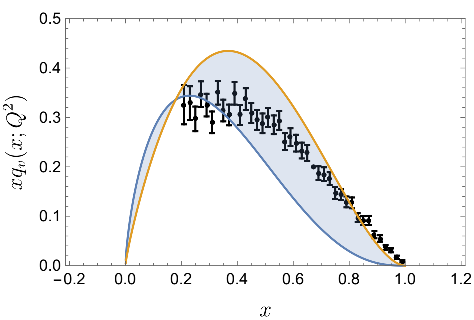

Fig. 3. Top left: The pion FF. The full line for GSWL2 and the dashed one for GSWL1. Top right: The pion TFF. Dashed line for GSWL2 and dot-dashed line for GSWL1. Bottom: The pion PDF evaluated at $Q^2 = 27$ GeV^2 within the GSWL2 parametrization. All data references are included in Ref. [5].

parametrizations lead to very good description of the spectrum. For the mean pion radius (0.67 ± 0.01 fm from experiment), we got 0.67 ± 0.03 fm (GSWL1) and 0.70 ± 0.05 fm (GSWL2). In Figs. 2–3, we show the calculations of the form factor (FF) of the distribution amplitude (DA), the transition form factor (TFF), and the parton distribution function (PDF). As one can see, very good agreements have been found.

6. Glueball–meson mixing

In Refs. [3, 4], a strategy to evaluate the mixing condition between scalar gluballs and mesons is shown. We consider a holographic light-front (LF) representation of the EoM in terms of the Hamiltonian [6] $H_{\rm LF}|\Psi_k\rangle = M^2|\Psi_k\rangle$ and a two-dimensional Hilbert space generated by a meson and a glueball states, $\{|\Psi_m\rangle, |\Phi_g\rangle\}$. Mixing occurs when the Hamiltonian is not diagonal in the subspace. Since we fixed the meson spectrum to the experimental values, $|\Psi_{\rm phy}\rangle$ represents a physical meson state while we have fixed the glueball spectrum to the lattice values. Thus, $\langle\Psi_{\rm phy}|\Phi_g\rangle$ represents the mixing probability which is proportional to the overlap of these two wave functions. We predict the existence of almost pure glueball states, in the scalar sector, in the mass range above 2 GeV.

7. Conclusions

In this contribution, we presented predictions of the GSW model. We showed that a large amount of experimental data have been described with only two parameters. For the pion, the SW dilaton has been properly modified to describe the chiral symmetry breaking in the model. Also in this case, the comparison with data of various quantities is quite good. We conclude by remarking on the predicting power of the model.

This work was supported by the STRONG-2020 project of the European Unions Horizon 2020 research and innovation programme under grant agreement No. 824093. The author thanks the organizers of the *Excited QCD 2022* workshop.

REFERENCES

[1] M. Rinaldi, V. Vento, *Eur. Phys. J. A* **54**, 151 (2018).
[2] M. Rinaldi, V. Vento, *Phys. Rev. D* **104**, 034016 (2021).
[3] M. Rinaldi, V. Vento, *J. Phys. G: Nucl. Part. Phys.* **47**, 055104 (2020).
[4] M. Rinaldi, V. Vento, *J. Phys. G: Nucl. Part. Phys.* **47**, 125003 (2020).

[5] M. Rinaldi, F.A. Ceccopieri, V. Vento, *Eur. Phys. J. C* **82**, 626 (2022).

[6] S.J. Brodsky, G.F. de Teramond, *Phys. Lett. B* **582**, 211 (2004).

[7] A. Karch, E. Katz, D.T. Son, M.A. Stephanov, *Phys. Rev. D* **74**, 015005 (2006).

[8] E. Folco Capossoli, H. Boschi-Filho, *Phys. Lett. B* **753**, 419 (2016).

[9] J. Erlich, E. Katz, D.T. Son, M.A. Stephanov, *Phys. Rev. Lett.* **95**, 261602 (2005).

[10] P. Colangelo *et al.*, *Phys. Rev. D* **78**, 055009 (2008).

[11] V. Vento, *Phys. Rev. D* **73**, 054006 (2006).

[12] V. Vento, *Eur. Phys. J. A* **52**, 1 (2016).

[13] G.F. de Teramond, S.J. Brodsky, *Phys. Rev. Lett.* **94**, 201601 (2005).

[14] P. Colangelo, F. De Fazio, F. Jugeau, S. Nicotri, *Phys. Lett. B* **652**, 73 (2007).

[15] E. Folco Capossoli *et al.*, *Chinese Phys. C* **44**, 064104 (2020).

[16] A.V. Sarantsev, I. Denisenko, U. Thoma, E. Klempt, *Phys. Lett. B* **816**, 136227 (2021).

[17] E. Klempt, *Phys. Lett. B* **820**, 136512 (2021).

[18] H. Boschi-Filho, N.R.F. Braga, H.L. Carrion, *Phys. Rev. D* **73**, 047901 (2006).

[19] F.J. Llanes-Estrada, P. Bicudo, S.R. Cotanch, *Phys. Rev. Lett.* **96**, 081601 (2006).

[20] Y. Kim, J.-P. Lee, S.H. Lee, *Phys. Rev. D* **75**, 114008 (2007).

[21] S.S. Afonin, I.V. Pusenkov, *Phys. Lett. B* **726**, 283 (2013).

[22] M.A. Martín Contreras, A. Vega, S. Cortes, *Chin. J. Phys.* **66**, 715 (2020).

[23] S. He, M. Huang, Q.-S. Yan, Y. Yang, *Eur. Phys. J. C* **66**, 187 (2010).

[24] Y. Li, J.P. Vary, *Phys. Lett. B* **825**, 136860 (2022).